VI. MICROWAVE ELECTRONICS[*]

Prof. L. D. Smullin
Prof. H. A. Haus
A. Bers
R. M. Bevensee

P. Chorney
K. W. Cooper, Jr.
H. W. Fock[†]

C. Fried
T. Goblick
A. Saharian
A. Zacharias

RESEARCH OBJECTIVES

The work of the Microwave Tube laboratory will be concerned with the following problems:
1. High-power tube research.
2. Noise in electron beams.
3. Plasma oscillation phenomena.
4. Microwave circuit theory and design techniques.
5. Parametric amplifiers.

The first four programs are a continuation of work that has long been in progress here. The work on parametric amplifiers has been undertaken in response to two diverse stimuli: interest in the basic theoretical problems and the promise of obtaining virtually noiseless parametric amplifiers.

1. High-Power Tubes

We plan to complete assembly and tests for the hollow-beam, stagger-tuned, L-band klystron. The future program will depend largely upon the test results. If the results are encouraging, one of the next important problems will be that of the electron gun.

Electron gun. The present tube uses a confined-flow parallel-beam gun that imposes very severe current-density problems on the cathode. Some means of obtaining a "converging" hollow beam will have to be developed. We are making preliminary studies of the Brillouin magnetron injection gun as a possible solution to this problem.

Transition between klystrons and traveling-wave tubes. A better understanding of the relationship between these two types of amplifier is needed. We plan to work on the problem of understanding what happens as the coupling between adjacent cavities is increased from zero (klystron) to a value that is large enough to disturb their resonant frequencies (traveling-wave tube).

2. Noise in Electron Beams

Present theoretical results indicate plainly that the ultimate noise performance of traveling-wave amplifiers is established by conditions at the cathode and virtual cathode. We propose to look into the problem of controlling the conditions at the virtual cathode in order (for example) to increase the Π/S ratio. We also plan to study more carefully what happens to noise at frequencies around the plasma frequency of the virtual cathode. In this problem both experimental and theoretical work will be necessary. Many of the techniques developed in this laboratory will be used in the experimental work for the measurement of the noise constants Π and S.

3. Plasma Oscillations

During the past year we have learned a good deal about the theoretical behavior of some ideal plasma systems. Our experimental results, however, have shown only a qualitative resemblance with theory. Thus, it seems clear that there must be some basic difference between the idealized model on which the theory is based and the actual experimental system. Our objective will be to bring the two together: (a) by making

---

more realistic assumptions about the theoretical model; and (b) by making the experimental model more like the ideal model.

4. Microwave Circuits and Slow-Wave Structures

A coupling-of-modes theory has been developed for the analysis of propagation along periodic structures. This analysis was convenient for obtaining a good approximate Brillouin diagram for periodic structures. It also provided a field-basis for the approximate equivalent circuit of a periodic structure. An attempt will be made to derive the formalism from a variational principle. The variational principle will provide a check on the accuracy of approximations.

5. Parametric Amplifiers

A general power theorem has been derived for parametric amplifiers that employ longitudinal electron beams and ferrites. On the basis of such a power theorem we can study the signal amplification and noise performance of parametric amplifiers. Parametric amplification will be studied along these lines.

L. D. Smullin, H. A. Haus

A. LOW-Q OUTPUT CAVITY FOR HOLLOW-BEAM KLYSTRONS[*]

The problem of designing a suitable output cavity for a wideband klystron has given us much trouble, but the present design seems to satisfy most of our requirements. The principal requirements are:

1. The bandwidth of the output cavity should be sufficiently wide so that advantage can be taken of the full electronic bandwidth of the tube.

2. The cavity should present an impedance to the beam that will allow the maximum ac power to be extracted from the beam.

Since beam size and gap length are prescribed by other considerations, the second requirement is usually the stronger and establishes the bandwidth. When low-impedance (high-perveance) beams are used, the desired gap impedance is very low, and the coupling to the load very strong. This leads to the next problem, that of distortion of the gap electric field by the coupling system (loop or iris). It is relatively easy to couple a cavity as tightly as desired; but most systems seriously distort the gap field, and thus reduce the effective coupling to the beam. The coaxial probe system described in the Quarterly Progress Report of April 15, 1957, page 46, has been studied further with the aid of field plots made in an electrolytic tank. There was a considerable amount of radial distortion caused by the probe.

The scheme that will be described arose from an attempt to use several weak couplings to the cavity, disposed symmetrically about the gap, as far from the gap as possible. Multiple-loop couplings with equal path-length interconnections, as shown in Fig. VI-1, were used. It can be shown that if all corresponding arms are of equal length and characteristic admittance, and if equal amplitude waves are excited at all
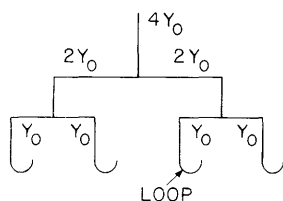
Fig. VI-1. Multiple-loop coupling system.

loops, there will be no standing waves in the system. Figure VI-2 shows a schematic drawing of the proposed design; Fig. VI-3 is a cross section of the proposed mechanical design. The system was tested with four loops that were not interconnected, but with each connected to its own matched load. The loaded Q of the system was 6. The R/Q value of the unloaded cavity had previously been measured as 70. If this value of R/Q still applied to the loaded cavity, the impedance at the gap should have been 420 ohms. The gap impedance was determined from a measurement of the transmission loss with a known rf resistance shunted across the cavity gap, as indicated schematically in Fig. VI-4. The resistance was made by putting a coating of Aquadag on a thin polystyrene tape. Each loop and its associated load presents a transformed conductance G' at the gap. The transmission of the cavity is

$$T = \frac{P_T}{P_{available}} = \frac{4G'^2}{(4G' + G)^2}$$

if we assume a lossless cavity. The measurement gave the following values:

G	T	4G'
0	-7.5 db	
$\frac{1}{500}$	-12.9 db	$\frac{1}{600}$

Since the transmission for G = 0 was -7.5 db instead of -6 db, it is evident that the loops were not all of equal size. It is apparent, however, that the R/Q value stays nearly constant in the whole range from $Q_L \approx \infty$ to $Q_L = 6$.

L. D. Smullin, K. W. Cooper, Jr., H. W. Fock

B. PROPAGATION IN A CIRCULAR WAVEGUIDE LOADED WITH A NONDRIFTING PLASMA

In our search for a theoretical explanation of electron-stimulated ion oscillations (1, 2) we studied the problem of propagation in a drift tube loaded with trapped ions. The effects of the electron beam were completely ignored and we assumed that the beam served only to neutralize the dc space charge. The model that was studied consisted of an infinitely long circular pipe of radius a, concentric with a cylindrical cloud of ions that has a radius b in the absence of an excitation (Fig. VI-5). The ion cloud was assumed to have a uniform dc volume charge density ρ_o. The effect of a
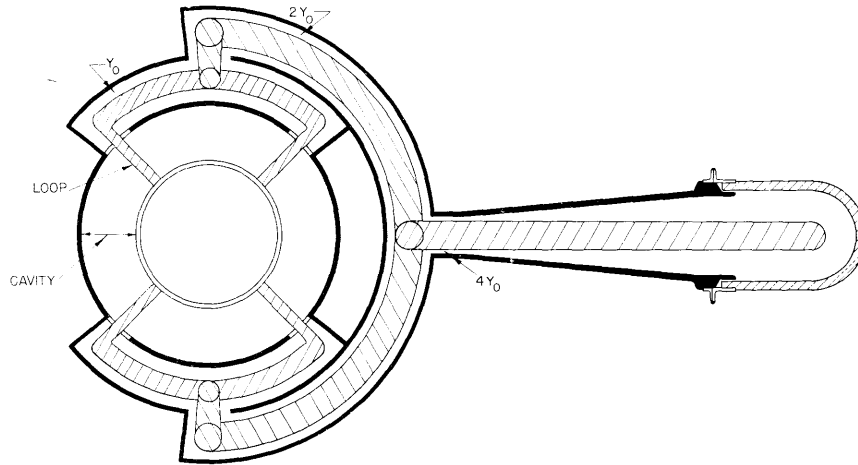
Fig. VI-2. A stage in the mechanical development of the four-loop coupled cavity.
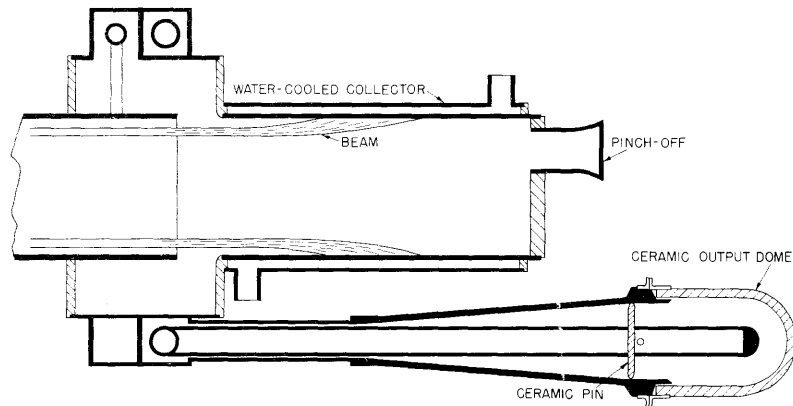
Fig. VI-3. Proposed four-loop coupled output cavity for use with hollow-beam klystron.
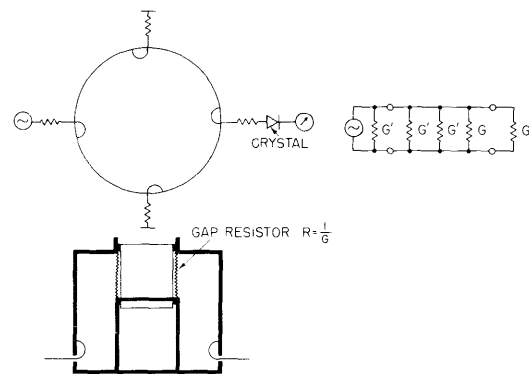
Fig. VI-4. Equivalent circuit and scheme for measuring R/Q of four-loop cavity.

longitudinal focusing magnetic field $\vec{B}_O = \vec{i}_z B_O$ was considered in the analysis.

The following equations describe rf excitation within the plasma:

$$\nabla^2 \vec{E}^I + k^2 \vec{E}^I = j\omega\mu\vec{J} + \nabla(\nabla \cdot \vec{E}^I) \tag{1}$$

$$\vec{J} = \rho_O \vec{v} \tag{2}$$

$$j\omega m\vec{v} = q\left(\vec{E}^I + \vec{v} \times \vec{B}_O\right) \tag{3}$$

The superscript I refers to region I (the plasma). Equation 1 is the vector wave equation for electric field derived from Maxwell's equations; Eq. 2 is the small-signal relation between rf particle motion and rf current density; and Eq. 3 is the small-signal nonrelativistic force equation. We assumed that the electric-field configuration in the plasma is independent of θ and of the mathematical form:

$$E_z^I = AJ_0(\beta_r r)\, e^{-j\beta_z z} \tag{4}$$

$$E_r^I = BJ_1(\beta_r r)\, e^{-j\beta_z z} \tag{5}$$

$$E_\theta^I = CJ_1(\beta_r r)\, e^{-j\beta_z z} \tag{6}$$

This assumed configuration is consistent with Eqs. 1, 2, and 3. By working Eqs. 4, 5, and 6 through Eqs. 1, 2, and 3, we obtain the dispersion relation,

$$\left[-\beta_r^2 - \beta_z^2 + k^2\left(1 - \frac{\omega_p^2}{\omega^2}\right)\right]^2 \left(1 - \frac{\omega_p^2}{\omega^2}\right)$$

$$- \frac{\omega_c^2}{\omega^2}\left[-\beta_r^2 - \beta_z^2 + k^2\right]\left[-\beta_r^2 + \left(-\beta_z^2 + k^2\right)\left(1 - \frac{\omega_p^2}{\omega^2}\right)\right] = 0 \tag{7}$$

and the relations

$$\frac{C}{B} = \frac{\omega_c}{\omega}\frac{\omega_p^2}{\omega^2 - \omega_c^2}\frac{jk^2}{-\beta_r^2 - \beta_z^2 + k^2\dfrac{\omega^2 - \omega_p^2 - \omega_c^2}{\omega^2 - \omega_c^2}} \tag{8}$$

and

$$\frac{A}{B} = \frac{-j\beta_z\beta_r}{-\beta_r^2 + k^2\left(1 - \frac{\omega_p^2}{\omega^2}\right)} \tag{9}$$

where

$$\omega_p^2 = \frac{q\rho_o}{\epsilon_o m}, \quad \omega_c = \frac{qB_o}{m}, \quad k^2 = \omega^2\epsilon_o\mu_o$$

For reasonable values of ω_p and ω_c (approximately a few megacycles) and reasonable geometries (b and a, approximately a few centimeters), $k^2 \approx 0$ over a frequency range extending from zero to approximately one tenth the cutoff frequency of the empty wave-guide (approximately a few kilomegacycles). Hence, relations 7, 8, and 9 can be approximated in this range as follows:

$$\beta_z^2 = \frac{\omega^2\left(\omega_p^2 + \omega_c^2 - \omega^2\right)}{\left(\omega_p^2 - \omega^2\right)\left(\omega_c^2 - \omega^2\right)}\beta_r^2 \tag{10}$$

$$\frac{C}{B} = 0 \tag{11}$$

$$\frac{A}{B} = j\frac{\beta_z}{\beta_r} \tag{12}$$

Relations 11 and 12 suggest that in the plasma $\vec{E}^I \approx -\nabla V^I$, where

$$V^I = V_o J_o(\beta_r r)\, e^{-j\beta_z z} \tag{13}$$

Therefore, we can reformulate the problem for the low-frequency range and describe the fields by Eqs. 2 and 3 in conjunction with

$$\vec{E}^I = -\nabla V^I \tag{14}$$

and

$$\nabla^2 V^I = -\frac{\rho}{\epsilon_o} = \frac{\nabla \cdot \vec{J}}{j\omega\epsilon_o} \tag{15}$$

Relation 13 is consistent with Eqs. 2, 3, 14, and 15, and the dispersion relation (Eq. 10) can be rederived by working Eq. 13 through these equations. For high frequencies, $\omega \gg \omega_p$ and ω_c, the plasma looks like a vacuum.

In the low-frequency range, the fields in region II (the vacuum) are approximately described by

$$\vec{E}^{II} = -\nabla V^{II}$$

and by

$$\nabla^2 V^{II} = 0 \tag{16}$$

Applicable solutions to Eq. 15 are of the form

$$V^{II} = [AI_0(\beta_z r) + BK_0(\beta_z r)] e^{-j\beta_z z}$$

In the presence of an excitation the boundary between the plasma and the vacuum ripples (Fig. VI-6). By using the method introduced by Hahn (3), this ripple can be replaced by a charge sheet at $r = b$ (Fig. VI-7), the surface charge being $\sigma = \rho_0 \Delta b$, in which Δb is the change in the radius b caused by an excitation. The change in radius Δb is given by

$$\Delta b = \frac{v_r}{j\omega}\bigg|_{r=b}$$

Therefore we obtain

$$\sigma = \epsilon_0 \frac{\omega_p^2}{\omega_c^2 - \omega^2} E_r^I \bigg|_{r=b}$$

(The expression for surface charge can be derived by considering the divergence of the current in a small volume element of dimensions Δb, Δz, $b\Delta\theta$ at the edge of the plasma and by neglecting products of small-signal quantities.)

The boundary conditions that must be fulfilled are:

$$V^{II}(a) = 0$$

$$V^I(b) = V^{II}(b)$$

$$\epsilon_0 E_r^I + \sigma = \epsilon_0 E_r^{II}$$

From these boundary conditions, we find

$$V^{II} = V_0 J_0(\beta_r b) \frac{I_0(\beta_z r) - \dfrac{I_0(\beta_z a)}{K_0(\beta_z a)} K_0(\beta_z r)}{I_0(\beta_z b) - \dfrac{I_0(\beta_z a)}{K_0(\beta_z a)} K_0(\beta_z b)} e^{-j\beta_z z} \tag{17}$$

and the determinantal equation
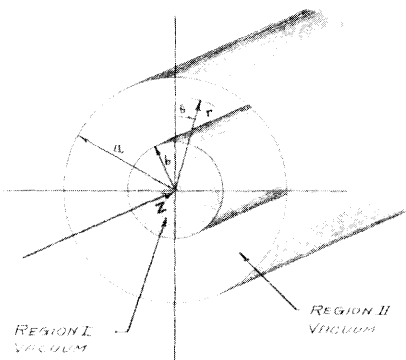
Fig. VI-5.   Circular waveguide with
cylindrical plasma.
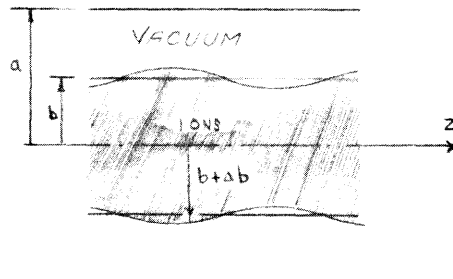
Fig. VI-6.   Ripple in plasma boundary.
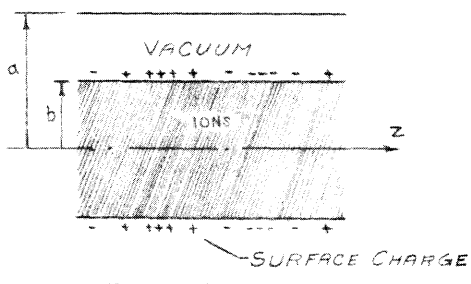
Fig. VI-7.   Surface charge replacing
ripple.
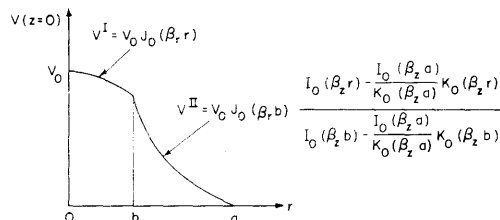
Fig. VI-8.   Transverse potential for
lowest radial mode of
first configuration.
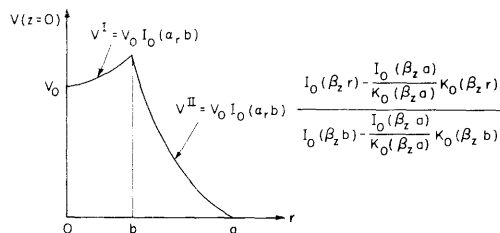
Fig. VI-9.   Transverse potential for second configuration.

$$\frac{\omega_p^2 + \omega_c^2 - \omega^2}{\omega_c^2 - \omega^2} \beta_r b \frac{J_1(\beta_r b)}{J_0(\beta_r b)} = \beta_z b \frac{I_0(\beta_z a) K_1(\beta_z b) + I_1(\beta_z b) K_0(\beta_z a)}{I_0(\beta_z a) K_0(\beta_z b) - I_0(\beta_z b) K_0(\beta_z a)} \tag{18}$$

It is also possible to have a different field configuration inside the plasma. The potential function

$$V^I = V_0 I_0(a_r r) e^{-j\beta_z z}$$

is also a solution to Eqs. 2, 3, 14, and 15 and yields the dispersion relation

$$\beta_z^2 = - \frac{\omega^2 \left(\omega_p^2 + \omega_c^2 - \omega^2\right)}{\left(\omega_p^2 - \omega^2\right)\left(\omega_c^2 - \omega^2\right)} a_r^2 \tag{19}$$

When the boundary conditions are matched, we obtain the determinantal equation,

$$-\frac{\omega_p^2 + \omega_c^2 - \omega^2}{\omega_c^2 - \omega^2} a_r b \frac{I_1(\beta_r b)}{I_0(\beta_r b)} = \beta_z b \frac{I_0(\beta_z a) K_1(\beta_z b) + I_1(\beta_z b) K_0(\beta_z a)}{I_0(\beta_z a) K_0(\beta_z b) - I_0(\beta_z b) K_0(\beta_z a)} \tag{20}$$

A sketch of a possible potential function of the first field configuration, i.e., the potential with the plasma variation $J_0(\beta_r r)$, is shown in Fig. VI-8. A sketch of the potential function of the second field configuration, i.e., the potential with the plasma variation $I_0(a_r r)$, is shown in Fig. VI-9.

For the first configuration, plots of β_z versus ω can be obtained from Eqs. 10 and 18. For $\omega_c < \omega_p$, propagation is obtained for $0 < \omega < \omega_c$ and for $\omega_p < \omega < \left[\omega_p^2 + \omega_c^2\right]^{1/2}$ (Fig. VI-10, solid curve). For $\omega_c > \omega_p$, waves propagate for $0 < \omega < \omega_p$ and for $\omega_c < \omega < \left[\omega_p^2 + \omega_c^2\right]^{1/2}$ (Fig. VI-11). An infinite number of θ-independent modes is obtained because of the repetitive nature of the left-hand side of Eq. 17.
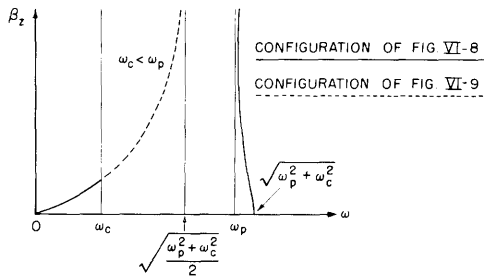
Fig. VI-10. ω-β diagrams for $\omega_c < \omega_p$, lowest radial mode.
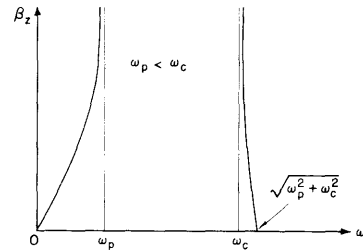
Fig. VI-11. ω-β diagram for $\omega_p < \omega_c$, lowest radial mode.

From Eqs. 19 and 20, plots of β_z versus ω can be obtained for the second configuration. For $\omega_c < \omega_p$, propagation is obtained in the band $\omega_c < \omega < \left[\left(\omega_p^2 + \omega_c^2\right)/2\right]^{1/2}$ (Fig. VI-10, dashed curve); there is only one such mode, since Eq. 20 is not repetitive. This type of propagation is not predicted if the ripple is neglected in the analysis, whereas the modes of the first configuration are predicted. For $\omega_c > \omega_p$, the second configuration does not propagate at all. [Calculated curves from R. Gould and A. W. Trivelpiece, California Institute of Technology, aided in the sketching of Figs. VI-10 and VI-11.]

P. Chorney

References

1. L. D. Smullin, C. Fried, and R. Bevensee, Electron-stimulated ion oscillations, Quarterly Progress Report, Research Laboratory of Electronics, M. I. T., April 15, 1957, pp. 51-53.

2. P. Chorney, Theoretical investigation of electron-stimulated ion oscillations, Quarterly Progress Report, Research Laboratory of Electronics, M. I. T., Oct. 15, 1957, pp. 30-35.

3. W. C. Hahn, Small signal theory of velocity modulated electron beams, Gen. Elec. Rev. 42, 258-270 (1939).

C. POWER RELATIONS IN PARAMETRIC, NONLINEAR MEDIA

Amplifiers that employ nonlinear media excited at a pump frequency f_p so as to provide gain at the signal frequency are called "parametric amplifiers." Manley and Rowe (1) derived some general relations that are fulfilled by powers that pertain to various frequencies and flow into a nonlinear capacitor. The small-signal form of the relations derived by Manley and Rowe has been extended to include longitudinal electron beams under nonlinear, parametric excitation. The small-signal form has also been generalized to include lossless gyromagnetic media with a magnetization $\overline{M}$ that satisfies the equation

$$\dot{\overline{M}} = -\gamma(\overline{M} \times \overline{H})$$

Both generalizations have been submitted for publication. Here, we shall only state the general theorems and briefly indicate some of their applications. Consider a longitudinal electron beam (confined by an infinite magnetic field) excited at a pump frequency, f_p, and modulated by a small signal at the signal frequency f_s. Denote the small-signal sideband pertaining to the frequency $mf_p \pm f_s$ by the subscript $mp \pm s$. Then, we have

$$\nabla \cdot \sum_{m=-\infty}^{\infty} \sum_{n=\pm 1} \left[\frac{n\overline{E}_{mp+ns} \times \overline{H}_{mp+ns}^*}{mf_p + nf_s} + \frac{nV_{mp+ns} \cdot J_{mp+ns}}{mf_p + nf_s} \right] = 0 \qquad (1)$$

where V and J are the complex small-signal amplitudes of the kinetic voltage and

49

current density. Equation 1 may be considered as a generalization of the small-signal kinetic-power theorem of Chu, to which Eq. 1 reduces if we disregard the pumping excitation and set all terms equal to zero except those corresponding to m = 0. Note that the electromagnetic and kinetic power of all lower sidebands enters into Eq. 1 with a negative sign. Thus, for example, the excitation of a fast wave at a lower side-band frequency (which carries positive kinetic power in a conventional longitudinal beam amplifier) acts upon an excitation at an upper sideband frequency in a manner similar to a slow-wave excitation at an upper sideband frequency. This explains why coupling produced by the pump excitation between two fast electron-beam waves, one at an upper sideband, the other at a lower sideband, can lead to exponential growth, a result that can be obtained from the small-signal analysis of a special case (2).

The small-signal power relations for lossless gyromagnetic materials are

$$\nabla \cdot \sum_{m=-\infty}^{\infty} \sum_{n=\pm 1} \frac{n \overline{E}_{mp+ns} \times \overline{H}^*_{mp+ns}}{mf_p + nf_s} = 0$$

These power relations are entirely analogous to the relations that were proved by Manley and Rowe for lossless, nonlinear capacitors and inductors. It follows that devices containing nonlinear gyromagnetic materials are subject to exactly the same limitations as those contained in the original Manley-Rowe relations.

H. A. Haus

References

1. J. M. Manley and H. E. Rowe, Some general properties of nonlinear elements —
    Part I, General energy relations, Proc. IRE 44, 904-914 (1956).
2. C. F. Quate, private communication, 1957.

D. MODE COUPLING IN A PERIODICALLY LOADED TRANSMISSION LINE

This work is an extension of the coupling-of-modes formalism applied to periodic cavity chains that was presented by R. Bevensee in the Quarterly Progress Report of October 15, 1957, page 25. In order to evaluate the accuracy of the approximations that were used to make this formalism manageable, an actual periodic structure whose exact solution is known was analyzed by mode coupling. The results indicate the validity and usefulness, in general, of the mode-coupling approach.

A transmission line that is periodically shunted by lumped capacitance is a simple periodic structure for which the exact solution can be found. The structure is shown in Fig. VI-12. One of its peculiarities is that it possesses an infinite number of pass-bands and stopbands in which the free waves are either propagating or are attenuated.
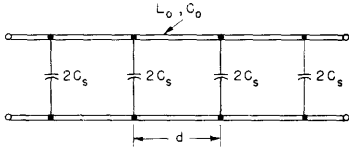
Fig. VI-12. Periodically loaded trans-
mission line.
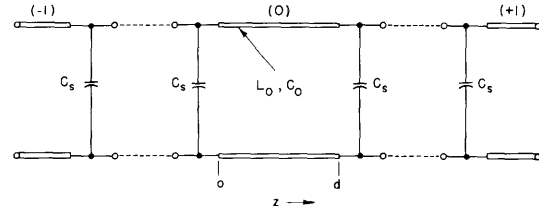
Fig. VI-13. Periodic structure broken
down into sections.

Each passband is bounded by a resonance of a section of the structure like that shown
in Fig. VI-13. The lower cutoff of each passband occurs when the length (d) of the
section is some integral number of half wavelengths, or at the resonances of a section
with short-circuited terminals. Hereafter, these will be called "short-circuit modes."
The upper cutoff frequency is the resonant frequency of a section with open-circuited
terminals which is affected by the shunt capacitors. These modes will be referred to
as the open-circuit modes.

A typical section of the periodic structure could be solved as a Sturm-Liouville
problem with the boundary condition that the voltage at the ends is zero, which will
give a complete set of orthogonal short-circuit modes. The section could also be solved
for the boundary conditions that current is zero at the ends, which will give a complete
set of orthogonal open-circuit modes. Either of these mode expansions is complete
and can be used to represent an arbitrary voltage and current distribution over the
section. Suppose that the voltage and current of the (0) section are written in terms of
the short-circuit expansions:

$$V_o(z) = \sum_n V_n E_n(z), \quad I_o(z) = \sum_n I_n H_n(z) \tag{1}$$

where $E_n(z)$ and $H_n(z)$ are the voltage and current distributions of the nth mode, and
V_n and I_n their complex amplitudes. The voltage and current of the preceding (-1)
section are:

$$V_-(z) = \sum_n V_n e^{j\phi} E_n(z), \quad I_-(z) = \sum_n I_n e^{j\phi} H_n(z) \tag{2}$$

by Floquet's theorem for a wave propagating from left to right on the structure.

In order to obtain the solution for a general voltage and current distribution in the
(0) section of the periodic structure at a certain applied frequency, it is necessary to
evaluate the mode amplitudes V_n and I_n. To do this, the effects of the adjacent (-1)

51

and (+1) sections are represented in the transmission line equations as driving terms. Then those equations can be solved for the (0) section. The individual sections are thus coupled together to form the periodic structure, and the driving effects of the adjacent sections can be represented by voltage or current generators at both ends of the (0) section.

If the driving terms are expressed as short-circuit mode expansions, we find that these modes do not couple to the short-circuit expansions of the (0) section, since they both satisfy the same boundary conditions. Therefore the open-circuit mode expansions are used for the driving terms of the short-circuit expansion and an infinite set of coupling equations results. Another set of coupling equations can be found by expressing the voltage and current of the (0) section in open-circuit expansions and the driving terms in short-circuit expansions. There are enough equations to evaluate all amplitudes in all mode expansions and thus to solve the problem formally.

Having both kinds of expansions for the voltage and current is advantageous, since the short-circuit expansion for voltage is not uniformly convergent at the ends of a section; nor is the open-circuit expansion for current uniformly convergent at the ends. Hence, if the infinite summations are to be truncated with a finite number of terms, the short-circuit expansion for current would be used for rapid convergence everywhere, and the open-circuit expansion for voltage would be chosen. These expansions converge rapidly, even at the extreme ends of the section, which, in general, have a finite voltage and current.

If the shunt loading is very heavy, the passbands are very narrow and the voltage and current distributions closely resemble those of the short-circuit and/or open-circuit resonant modes that mark the cutoff frequencies of that passband. The simplest approximation, then, is to postulate that all other modes except these two affect the solution to a negligible extent, and so they are omitted. All of the infinite summations reduce to single terms, and a first-order approximation for the propagation characteristics can be found. This approximation (called the single-mode-pair approximation) leads to a simple relation for ϕ, the phase shift per section of a propagating wave, in terms of the frequency ω. This is called the "frequency equation," and it is written

$$\omega^2 = \frac{\omega_{sn}^2 + \omega_{on}^2}{2} \pm \frac{\omega_{sn}^2 - \omega_{on}^2}{2} \cos \phi$$

where ω_{sn} and ω_{on} are, respectively, the short-circuit and open-circuit resonant frequencies of the nth passband. The plus sign of the plus-and-minus combination is used if the voltage distributions of the modes are antisymmetric in the section; the minus sign is used for symmetric voltage modes.

The next better approximation would be to acknowledge the existence of modes associated with the nearby passbands and write the coupling equations for two-mode
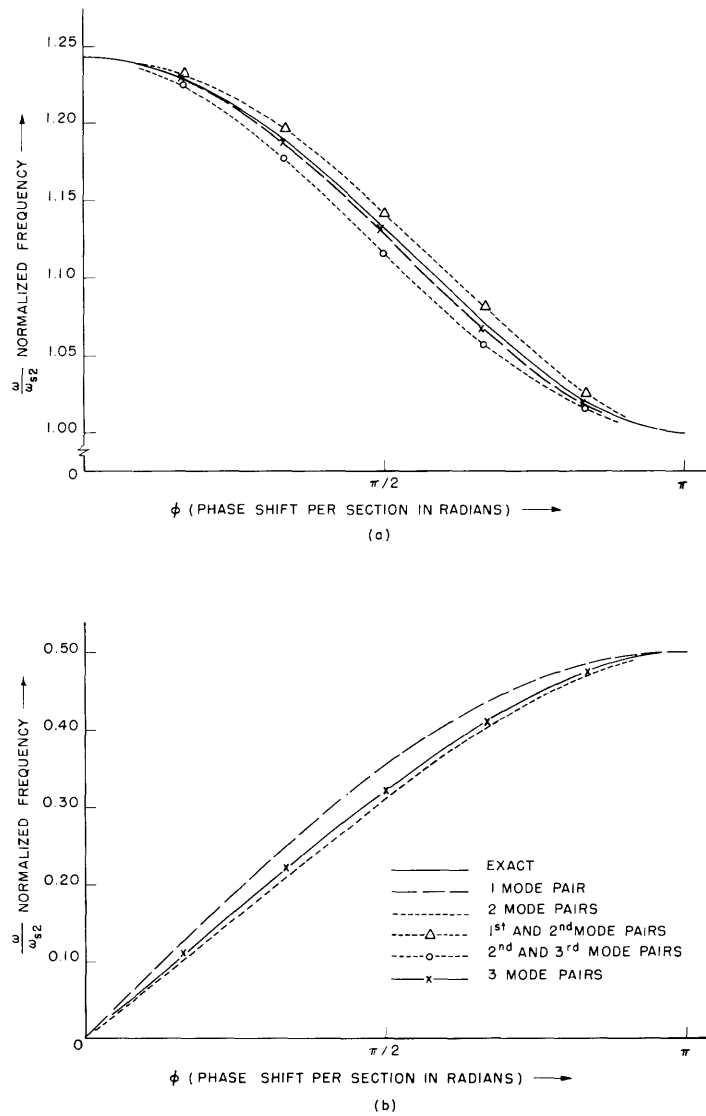
Fig. VI-14. Brillouin (ω versus β) diagram for the periodically loaded transmission line; ω_{s2} is the half-wave resonant frequency of a section.

pairs or even three-mode pairs. That is, in studying the nth passband, the coupling equations would be written to include the modes of the $n-1$ and $n+1$ passbands.

Such approximations were carried out for the periodically loaded transmission line of Fig. VI-12, and the results for one-, two-, and three-mode-pair approximations are plotted, together with the exact solution found by other methods. The propagation characteristics of the low passband, which begin at dc, and of the second passband are plotted in Fig. VI-14. The results indicate that the higher-order approximations converge to the exact solution rapidly, even when the shunt loading is not very heavy. (The bandwidth of the second passband is approximately 22 per cent.)

Note that the two-mode-pair approximations for the second passband are poorer than the single-mode-pair approximation. In analyzing the nth passband of a periodic structure, the $n - 1$ and $n + 1$ passbands contribute comparative effects; thus the next higher approximation that should be used after the single-mode-pair case would be the three-mode-pair approximation. The two-mode-pair approximation destroys the symmetry of the problem. For the passband beginning at dc, any additional modes coupled into the system give more accurate results, since there is no symmetry to preserve.

T. Goblick